Screen-Printed Electrochemical Biosensor for the Detection of Bacteriophage of *Lactococcus Lactis* for Dairy Production

Stefano Bonaldo, *Member, IEEE*, Erica Cretaio, Elisabetta Pasqualotto, Matteo Scaramuzza, *Member, IEEE*, Lara Franchin, Sara Poggi, and Alessandro Paccagnella, *Senior Member, IEEE*

***Abstract*—In the dairy industry, the spreading of phages of *Lactococcus lactis* (LL) prevents the proper lactic fermentation, causing waste of contaminated products and economic losses. This work presents a cheap biosensing method for rapidly detecting the LL phages. The detection is based on live LL bacteria covering the sensor electrodes, whose electrical response is measured by electrochemical impedance spectroscopy (EIS). Solutions contaminated by phages induce bacteria lysis, clearly reducing the bacteria coverage over the electrodes and leading to evident parametrical shifts in the charge transfer resistance and in the impedance phase at 400 Hz. Experimental tests with laboratory contaminated samples confirm the better detection capability of screen-printed gold sensors compared to the interdigitated gold electrodes. Two measurement protocols, called spill-out and drop-in methods, are evaluated to optimize the sensor detection capability and time. The EIS results are compared with optical absorbance measurements at 600 nm, in order to validate the proposed detection method with 10^7-PFU/mL phages and with a detection time of about 5 h. Finally, the proposed method is tested successfully with milk-based solutions. Evident shifts between phage-contaminated and non-contaminated sensors are measured in the charge transfer resistance of more than one order of magnitude with impedance phase differences of 43°.**

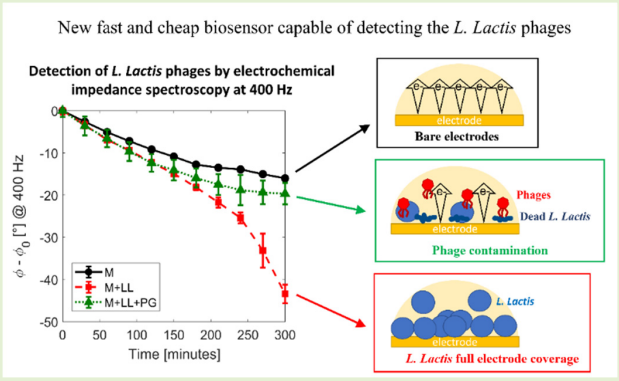

***Index Terms*— Electrochemical biosensor, electrochemical impedance spectroscopy (EIS), impedance phase, Lactococcus lactis (LL), phage, resistance to charge transfer.**

I. Introduction

THE dairy industry requires the continuous monitoring of the presence of dangerous pathogens along the production chain and in its final products. Fast pathogen detection allows to isolate contaminated lots and proceed selectively with sanitation protocols. The proliferation of the phages of *Lactococcus lactis* (LL) in milk lots is one of the major concerns for the dairy sector. The LL phages prevent the proper lactic fermentation, thus leading to inevitable waste of the contaminated products and to economic losses [1], [2]. At the state of the art, the most common detection methods of phages rely on microbiological laboratory tests, as the real-time polymerase chain reaction (PCR) and multiplex PCR [3]. These methods are time-consuming, expensive, and complex, as they require equipped laboratories (mostly located far from the dairy production sites), primers and reagents, and trained personnel [4]. As a consequence, the relatively high cost of these tests induces the industries to adopt recurring sanitation protocols, while the delay of the microbiological test results may cause the loss of multiple milk lots.

A valid alternative to the microbiological tests is the development of an electrochemical biosensor for the rapid and cheap detection of phages [5], [6]. In the last years, different electrochemical biosensors have been developed for sensing analytes in the dairy industry [7], [8]. For example, an electrochemical biosensor was developed for monitoring the

Manuscript received 11 January 2023; accepted 27 January 2023. Date of publication 8 February 2023; date of current version 14 March 2023. The associate editor coordinating the review of this article and approving it for publication was Prof. Jeong Bong Lee. *(Corresponding author: Stefano Bonaldo.)*

Stefano Bonaldo, Lara Franchin, Sara Poggi, and Alessandro Paccagnella are with the Department of Information Engineering, University of Padova, 35131 Padua, Italy (e-mail: stefano.bonaldo@unipd.it).

Erica Cretaio and Elisabetta Pasqualotto are with ARCADIA s.r.l., 35132 Padua, Italy.

Matteo Scaramuzza is with the ARC-Centro Ricerche Applicate, 35132 Padua, Italy.

Digital Object Identifier 10.1109/JSEN.2023.3242107

presence of lactate in milk, which indicates the proper bacterial fermentation, allowing the evaluation of the freshness and quality degree of products [9]. Other works proposed biosensors to monitor the quantity of antibiotic in milk [10], [11] and to detect infections of dangerous bacteria [12], [13], [14], [15], [16].

It is worth noting that phages have been typically used in the biosensing as a recognition element [17]. In [18], the E2 phages immobilized on the working electrode surface were used for the selective binding to detect the *Salmonella* bacteria. On the other hand, only few works have explored biosensing approaches for the detection of the phages. In [19], an electrochemical biosensor sensitive to the bacteriophage *PhiX174* of *Escherichia coli WG5* was developed on screen-printed electrodes, basing the detection on the formation of bacterial biofilms. The biosensor measured the impedance imaginary component at low frequency, which was sensitive to the presence of bacteriophages in the milk solution under test. In [20], an electrochemical biosensor for the LL phages was developed on inkjet-printed interdigitated electrodes. The biosensor was based on measuring the parametrical shifts of the double layer capacitance and of the interdigitated capacitance in standard phosphate buffered solutions (PBSs).

II. Materials and Methods

A. Chemicals

The chemicals were of analytical grade. The water was filtered and deionized to ultrapure milli-Q water (MQ, filtered at 0.22 μm with conductivity <2000 μS/cm), while the milk was commercial off-the-shelf milk. The M17 broth, purchased from HiMedia Laboratories, was dissolved in MQ, and it was used as a culture medium for the growth of the LL. Phages were stored in a specific phage buffer (PB) prepared with 100-mM NaCl, 8-mM $MgSO_4$, and 50-mM Tris-HCl at pH 7.5.

Potassium hexacyanoferrate III ($K_3[Fe(CN)_6]$) and potassium hexacyanoferrate II ($K_4[Fe(CN)_6]$) trihydrate were purchased from Sigma Aldrich and were used as a redox couple ($Fe(CN)_6^{3-}$/$Fe(CN)_6^{4-}$) for the electrochemical measurements. The $Fe(CN)_6^{3-}$/$Fe(CN)_6^{4-}$ solutions (called FeCN solutions for brevity) were prepared at 10 mM by dissolving the potassium hexacyanoferrate III and potassium hexacyanoferrate II directly in the M17 broth.

B. Biological Elements

The LL and its *Bacteriophage P008* were provided by DSMZ, Germany, as a representative for infection of cultures in milk of dairy industries.

Preliminary tests aimed to the evaluation of the bacterial growth into the M17 broth (ideal condition) and into the other solutions used during the electrochemical tests, i.e., FeCN and PB. The LL cultures were tested in the solutions of M17, 10-mM FeCN in M17, 80-μL/mL PB in M17, and 10-mM FeCN + 80-μL/mL PB in M17. The LL growth was evaluated by measuring the optical density (OD) of solutions placed in proper cuvettes through the spectrophotometer ONDA, model UV-30 SCAN.

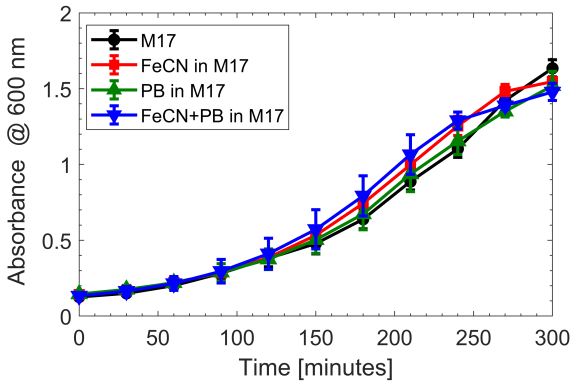

Fig. 1. Optical absorbance at 600 nm as a function of the time for sensors with different solutions starting from the same bacteria concentration.

Fig. 1 reports the optical absorbance measurements of the LL cultures in these different solutions at 30 °C at 600-nm wavelength, corresponding to the absorbance peak of the LL bacteria. All cultures of LL were diluted with the respective solutions to reach the initial OD of 0.1. All the curves are characterized by similar trends, demonstrating that the LL growth rate is not affected by the FeCN, which is required for electrochemical measurements, and by the PB. In general, the OD increases from 0.1 to 0.4 after 120 min, which is the bacteria doubling time. After 300 min, the OD settles at 1.5 reaching a stable value due to a gradual saturation of the bacterial growth.

C. Devices and Test Conditions

Two different biosensors based on screen-printed electrodes (DRPC223AT, DRP) and interdigitated electrodes (PW-IDEAU100, INTD) by Metrohm DropSens, Spain, were selected for the tests, as shown in Fig. 2(a). The DRP electrodes were screen-printed on a ceramic substrate (34 × 10 × 0.5 mm), with a conventional three-electrode configuration based on working (gold), counter (gold), and reference (silver) electrodes. The working electrode was a disk with 1.6-mm diameter. While, the INTD electrodes were produced on a transparent flexible plastic substrate (22.8 × 7 × 0.175 mm) and were designed in a two-electrode configuration made of gold. The width of the fingers and the interdigital gap were 100 μm. An external Ag/AgCl electrode was used as a reference.

All devices under test were enclosed into a hermetic customized cell, as shown in Fig. 2(b), to avoid undesired solution evaporation. The cell was 3-D-printed and contained a conic reservoir made in polydimethylsiloxane (PDMS) to confine the solution into a circular area of 8-mm diameter on the sensor surface. This cell was used to remove problems related to solution contamination and evaporation.

The biosensors were electrically characterized by using the electrochemical impedance spectroscopy (EIS). Preliminary cyclic voltammetry (CV) measurements were performed to obtain the redox standard potential E_0 of the electrochemical systems with a solution 10-mM FeCN in M17. The EIS measurements were performed by using the Solartron 1260A impedance analyzer and CH-404A potentiostat, as well as the

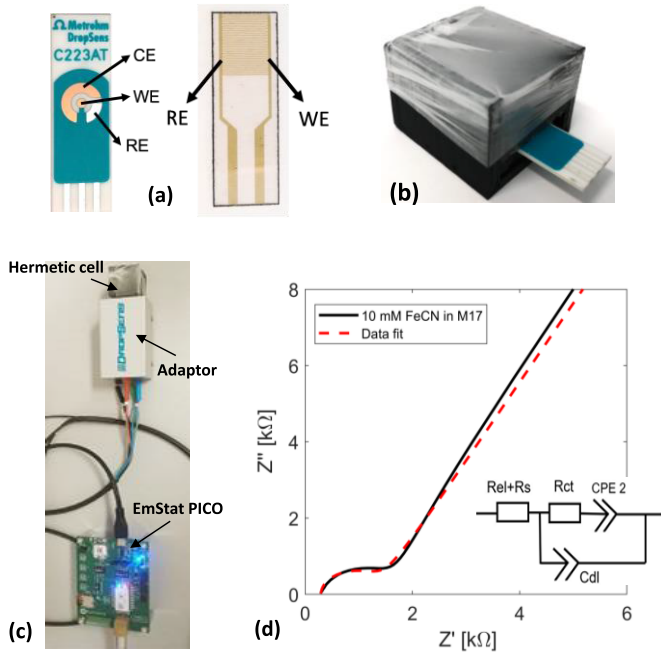

Fig. 2. (a) Electrodes: DRP (left) and INTD (right). (b) Hermetic electrochemical cell. (c) Experimental setup with the PalmSens EmStat PICO. (d) Nyquist diagram of EIS response of a fresh DRP sensor with 10-mM FeCN in M17 solution (black curve) and its fit through the equivalent circuit shown in the inset (red curve).

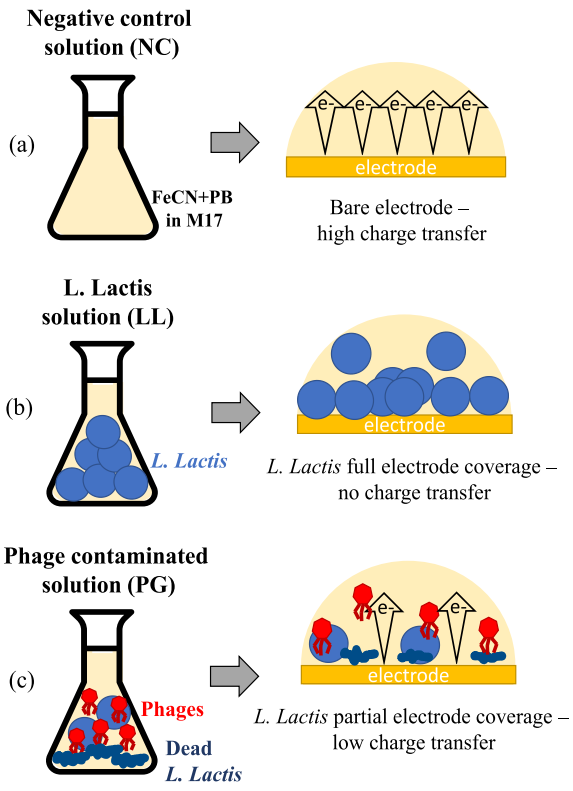

Fig. 3. Schematic representation of the proposed electrochemical sensing method for monitoring the presence of phage infection of the LL. (a) Only redox solution (FeCN + PB in M17) is characterized by a high charge transfer at the electrode/solution interface. (b) With LL proliferating, the surface of the electrode is fully covered by live LL, preventing the charge transfer. (c) Phages inhibit the LL bacteria proliferation, and the surface of the electrode is partially covered by live LL bacteria, allowing partial charge transfer.

PalmSens EmStat PICO, which is a portable and compact instrument [see Fig. 2(c)]. The EIS measurements were performed using the two-electrode configuration in a frequency range between 1 Hz and 100 kHz. The peak-to-peak amplitude of the ac signal was 10 mV, while the dc bias V_{dc} was 91 mV for the DRP electrode and 0 V for the INTD electrode, corresponding to the equilibrium redox potential E_0 retrieved by CV measurements.

After the measurements, the EIS responses were fit through the equivalent electric circuit shown in Fig. 2(d) (inset). The circuit was designed to have the solution/electrode resistance ($R_{el}+R_s$) in series to the parallel of a nonfaradic branch, which includes the double layer capacitance (C_{dl}), and a faradic branch, which includes the charge transfer resistance (R_{ct}) and a constant phase element (CPE2). Fig. 1(d) reports the EIS response of a fresh DRP electrode sensor measured with 10-mM FeCN in M17 solution. The equivalent circuit model fit well the experimental data, allowing the extrapolation of all the circuit parameters from the experimental measurements.

III. Proposed Detection Method

The working principle of the proposed detection method for the LL is based on the bacterial coverage on the electrodes, as illustrated in Fig. 3.

In Fig. 3(a), a solution composed by FeCN and PB in M17 is used for electrical characterization of bare electrodes. Under proper bias, the redox process controls the electric current flowing at the electrode/solution interface.

In Fig. 3(b), the solution contains LL bacteria, which proliferate. When a drop of LL solution is placed on the electrode surface, the living bacteria precipitate on the electrodes, fully covering the electrode surface. The bacteria coverage hampers the electric current to flow, thus inducing an increase in the charge transfer resistance.

In Fig. 3(c), the solution is contaminated with bacteriophages, which lead to death of a large number of bacteria cells and to the synthesis of other phages [21]. The resulting solution is highly contaminated by phages with low concentration of bacteria. The bacterial coverage of the electrode surfaces is partial and smaller than in Fig. 3(b), allowing higher current to flow. As a consequence, the charge transfer resistance decreases in comparison with Fig. 3(b).

IV. Experimental Results

A. Electrode Selection

The choice of a suitable electrode is crucial to obtain good performance of the sensor. Hence, we tested the stability and the reproducibility of the electrochemical measurements over time and after different cleaning procedures using the screen-printed electrodes (DRP) and the interdigitated electrodes (INTD).

First, we evaluated the time stability of the electrodes when kept in contact with the FeCN + PB in M17 solution, by performing measurements every 30 min. Fig. 4 shows the Nyquist plot of the EIS curves of DRP and INTD electrodes

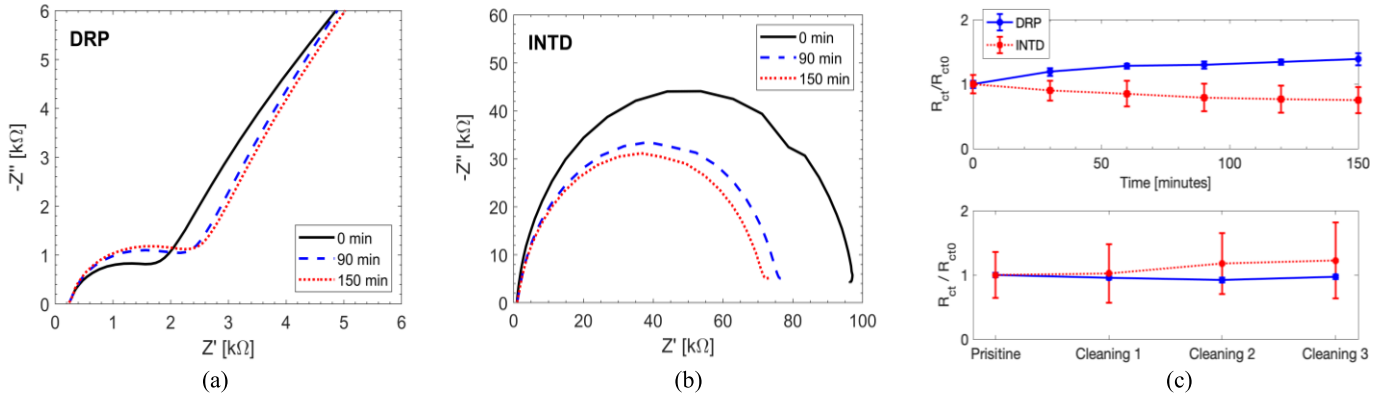

Fig. 4. Stabilities of (a) DRP and (b) INTD electrodes are evaluated with 10-mM FeCN in M17 as a function of time. (c) Normalized charge transfer R_{ct}/R_{ct0} is plotted as a function of the time (top) and of the cleaning sequence (bottom).

over an observation period of 150 min. In case of the INTD sensors, the Randles semicircle drifts toward lower values as time elapses, indicating a reduction of the charge transfer resistance. On the other hand, the DRP presents a 30% increase of R_{ct} after 150 min. The complete evolution over time of the normalized R_{ct} values for INTD and DRP electrodes is summarized in Fig. 4(c) (top), presenting in both cases a gradual shift versus time—DRP R_{ct} increases, while the INTD R_{ct} decreases with time. These results suggest choosing the INTD devices, as their R_{ct} variation is slightly smaller than for DRP sensors. Moreover, the DRP error bars (1σ standard deviation) are always much smaller than for INTD, clearly indicating that INTD electrodes present much better device-to-device repeatability when the time stability is considered.

Second, we evaluated the stability of the electrodes after subsequent cleaning protocols. Fig. 5 shows the normalized R_{ct} values for the fresh device and after subsequent cleanings, consisting in rinsing the electrodes with MQ and then drying at room temperature. The DRP electrodes show stable R_{ct} and small error bars, with limited effects produced by the cleanings. On the contrary, R_{ct} of INTD grows, exhibiting an ever-increasing trend and large standard deviations. The general higher device-to-device variability of the INTD devices may be attributed to the hand assembly of the PDMS-printed cells and differences in the plastic structures.

In general, the DRP electrodes proved to be more stable in time with less sample-to-sample variability than the INTD devices, as well as after multiple cleaning procedures. For these reasons, we selected the DRP electrodes for the following tests.

B. Detection of the Bacterial Growth

In this section, we present the experimental results for the growth detection of the LL. The bacterial solutions were prepared by adding 1200 μL of LL with an initial OD of 0.5, to 3000 μL of 20-mM FeCN in M17, and to 1800 μL of M17, in order to obtain a 10-mM FeCN in M17 solution with LL at final OD of about 0.1. The 10-mM FeCN solutions in M17 were the negative control (NC) solutions, which were prepared using 3000 μL of 20-mM FeCN in M17 and 3000 μL of M17.

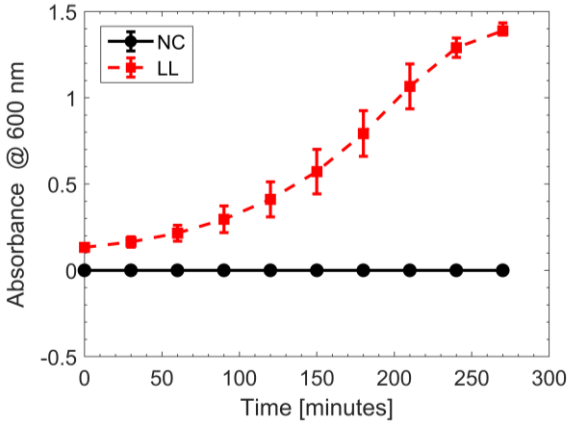

Fig. 5. OD at 600 nm as a function of the time for the NC solution, i.e., only 10-mM FeCN in M17 solution, and for the LL solution.

We detected the LL growth following two different protocols, called "spill-out" and "drop-in" methods. The drop-in method consisted in depositing a single drop of 90 μL of the test solution on the sensor electrodes. The solution drop was never removed throughout the entire set of measurements, till the end of the experiment after 270 min. On the contrary, the spill-out method consisted into depositing subsequent test solution drops of 90 μL only for the time needed for the electrical measurements with the sensor being rinsed with MQ after each measurement.

In both protocols, when the 90-μL drop was deposited on the sensors, the EIS response was measured after 15-min waiting time, which was necessary for the precipitation of the bacteria in solution on the electrode surface. Every 30 min, the same procedure was repeated for each sensor, reaching a maximum observation time of 270 min. The same protocol was applied to the control solution.

The growth of the LL in the solution was also measured through optical absorbance measurements, which were performed just before the electrochemical ones. Fig. 5 presents the OD values as a function of the time. For the LL solution, the OD increases due to the proliferation of the LL bacteria, likely approaching a plateau value over 1.4 at 270 min. On the other hand, the OD value of the NC solutions remains unchanged, around 0, along all the duration of the experiment, indicating absence of undesired contaminations.

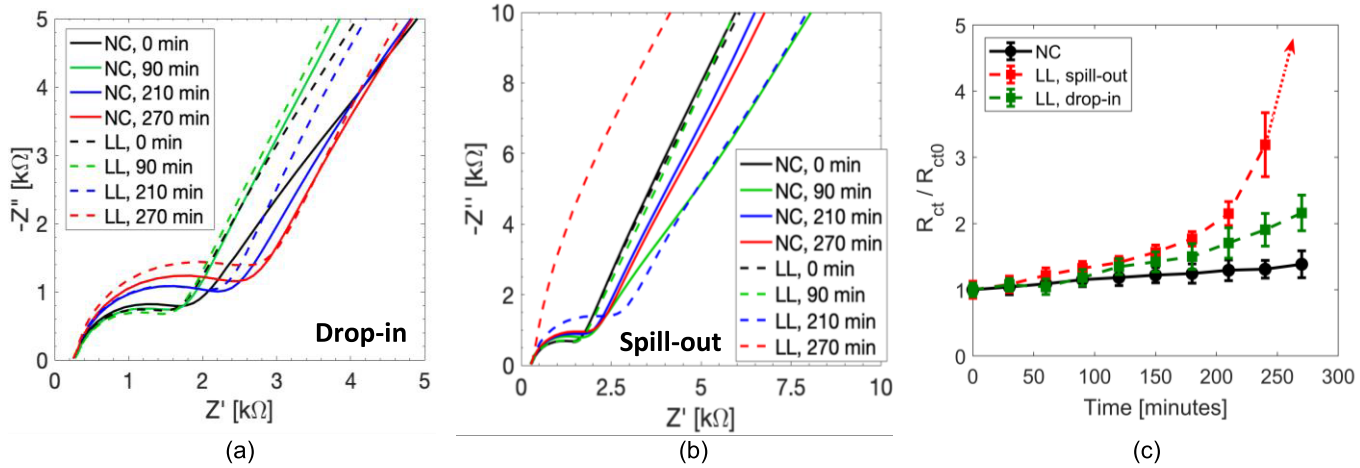

Fig. 6. EIS responses of sensors measured with 10-mM FeCN in M17 solution without NC and with LL. (a) Nyquist diagram obtained from the drop-in method. (b) Nyquist diagram obtained from the spill-out method. (c) Normalized value R_{ct}/R_{ct0} extrapolated by the measurements shown in (a) and (b).

Fig. 6 shows the EIS response of the sensors for NC and for LL at the time 0, 90, 210, and 270 min with the drop-in and spill-out methods. The starting time of the experiment is considered from the first performed measurement. For the drop-in method, the Nyquist diagram of Fig. 6(a) evidences similar variations between NC and LL. Instead, the spill-out method of Fig. 6(b) evidences large differences between the NC and the LL at 270 min. The LL sensors show a huge shift in the curve, caused by a large increase in R_{ct}. Meanwhile, the response of the NC sensors is practically stable, as expected, for the entire duration of the experiment.

Fig. 6(c) shows the normalized R_{ct} values over time. The spill-out LL curve starts increasing already after 60 min, in agreement with the OD values of Fig. 5. After 270 min, R_{ct} can no longer be extrapolated precisely, as its value increases by more than two orders of magnitude, meaning that the bacteria have covered the whole electrode surface, strongly hampering the current flow. The slight increase over time of R_{ct} for the NC sensors is negligible, since at time 270 min, the NC value is 1.2× the initial one, while LL in spill-out method is 100× times higher, granting an effective detection of the bacterial presence and proliferation on the electrode.

Comparatively, the drop-in method displays lower R_{ct} shifts than the spill-out method, indicating slower bacterial growth. This fact was confirmed by a visual inspection of the solution over the sensor after 270 min, when we observed almost no turbidity. The inhibition of the LL growth in the drop-in method is likely due to an excessive buildup of waste product released from the bacteria, or to the interactions between the metallic surface and the bacterial membrane that may lead to measurements artifacts, preventing proper phage detection.

In summary, the spill-out method proved to be more sensitive to the LL growth over time, as well as after multiple cleaning procedures. For this reason, we decided to use the spill-out method for further tests presented in Sections IV-C and IV-D.

C. Phage Detection

The bacteriophages were stored at −20 °C in their PB, whose composition was described in Section II-B. The phage

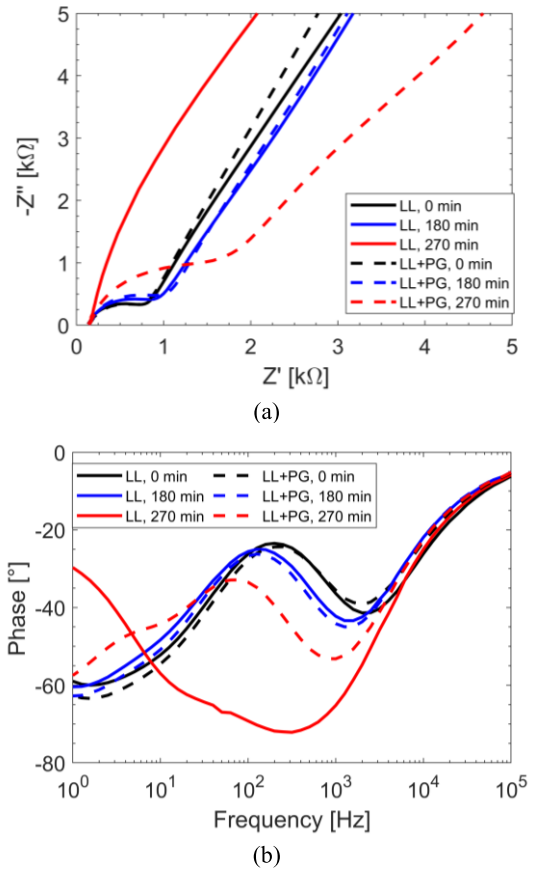

Fig. 7. EIS responses in ideal laboratory conditions for sensors with LL and with LL phage contamination (LL + PG). (a) Nyquist diagram. (b) Impedance phase versus frequency.

solutions were prepared at a phage concentration of 10^7 PFU/mL, typical of the dairy production [3]. Solutions of LL contaminated by phages (LL + PG solutions) were obtained by adding 480 μL of phages in PB to 1200 μL of LL at an OD of 0.5, to 3000 μL of 20-mM FeCN in M17, and to 1320 μL of M17, reaching a total final volume of 6 mL with 0.1 OD.

Fig. 7(a) shows the Nyquist curves of two different biosensors prepared with the LL (continuous line) and with LL contaminated by the phages (LL + PG, dashed line). At 0 and

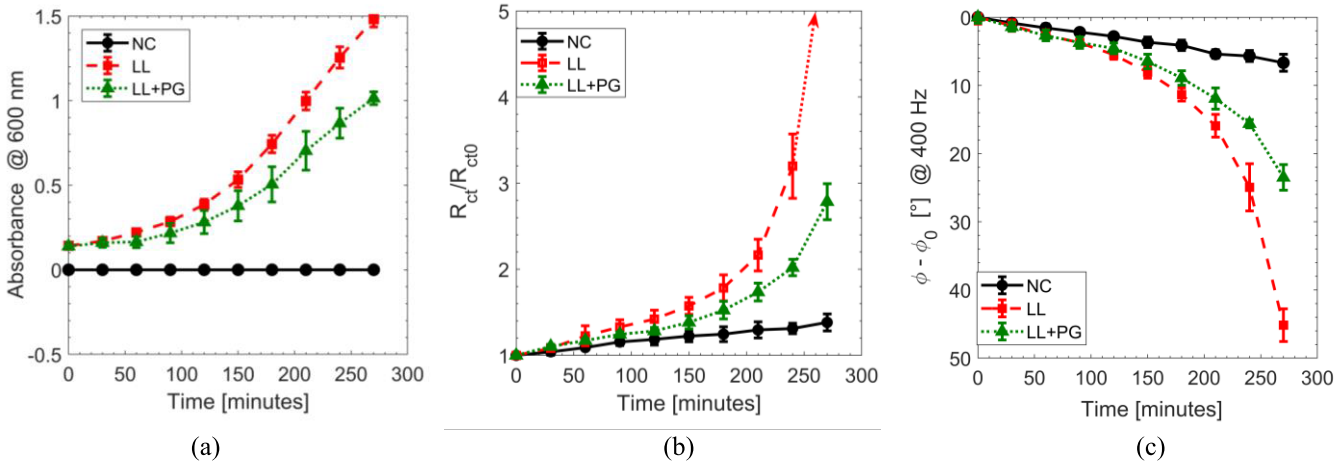

Fig. 8. Tests in ideal laboratory conditions for sensors with only buffer solution (NC), with LL, and with LL phage contamination (LL + PG). (a) Optical absorbance as a function of the time. (b) Normalized charge transfer resistance R_{ct}/R_{ct0} extrapolated by the EIS measurements. (c) Differential phase at 400 Hz extrapolated by the EIS measurements.

180 min, the LL and LL + PG curves nicely overlap each other. As the test time increases, large differences appear. After 270 min, the PG curve is still characterized by the typical semicircle at high/medium frequencies, even though the R_{ct} contribution has substantially increased. On the contrary, the LL curve exhibits a huge increase in the imaginary part of the impedance, as already observed in Fig. 6(b). This huge difference between LL and LL + PG sensors is related to the different effectiveness of the LL to cover the electrodes. The presence of phages in the solution induces the bacteria lysis, thus slowing down the bacteria growth and slowing down the R_{ct} increase.

Differences between LL and LL + PG sensors appear also when considering the impedance phase, as shown in Fig. 7(b). At 270 min, the phase curve becomes very distinguishable at frequencies <1 kHz. The highest difference between LL and LL + PG sensors is retrieved in the frequency range between 100 Hz and 1 kHz, due to the dominance of R_{ct} and of capacitive contributes, which strongly rely on the formation of bacterial layers on the electrode surface. Hence, a great discrimination parameter can be the phase values at 400 Hz, which requires a single-point frequency measurement. In the LL sensor (red continuous curve), the phase at 400 Hz is $-73°$ versus $-50°$ of the LL + PG sensor (red dashed curve). The phase difference between the contaminated and uncontaminated phage solutions is significant, as it is 23° at 270 min.

Fig. 8(a) shows the absorbance measurements for the NC, LL, and LL + PG solutions used for the EIS tests shown in Fig. 8(b) and (c). The NC absorbance is approximately stable around 0, meaning the absence of external undesired contamination. At times lower than 60 min, the difference between the LL and LL + PG curves is within the experimental error. At longer times, the curves start to separate, and the distance keeps increasing with the time. These results indicate that the bacteria growth rate of the LL solution is higher than the one of PG, as the phages activity slows down the bacterial growth without inhibiting it completely.

This difference clearly appears in the normalized R_{ct} of Fig. 8(b) and in the impedance phase at 400 Hz of Fig. 8(c). At

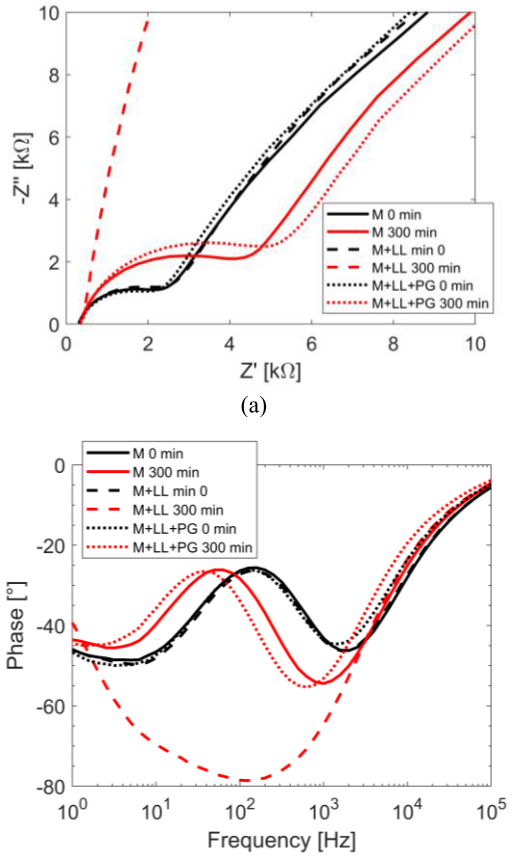

Fig. 9. EIS responses in treated-milk samples for sensors with only buffer solution in milk (M), with LL (M + LL), and with LL phage contamination (M + LL + PG). (a) Nyquist diagram. (b) Impedance phase versus frequency.

270 min, the normalized R_{ct} of LL + PG sensors increases to 2.8, consistent with a limited growth of the LL compared with LL sensors, where the normalized R_{ct} values surge. We remark that the bacterial growth observed through the electrochemical measurements is in good agreement with the trends deduced from the absorbance measurements.

Similar to R_{ct}, the impedance phases of LL and LL + PG sensors exhibit similar shifts before 180 min. As time

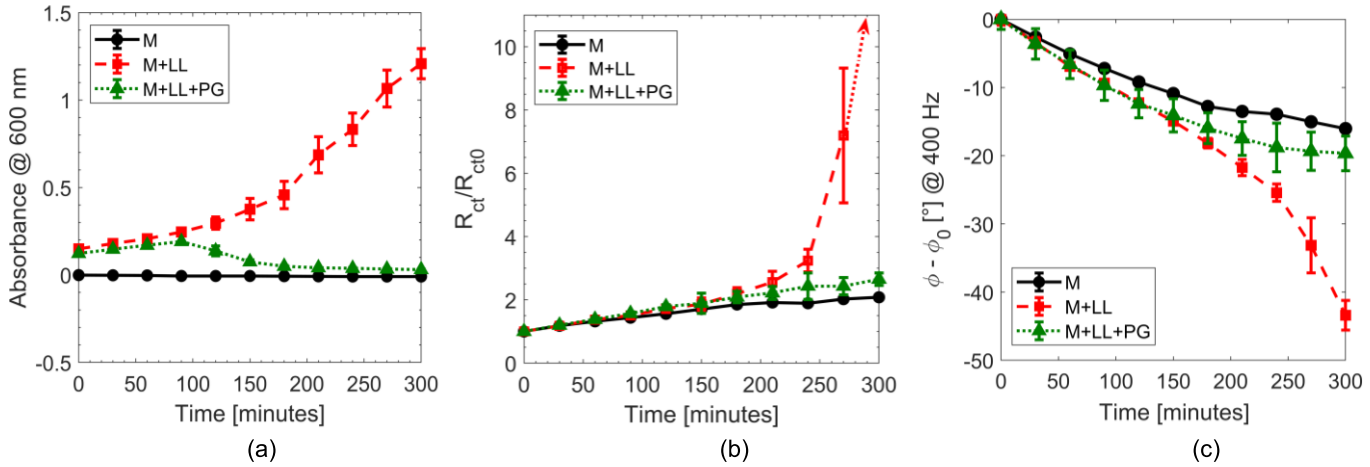

Fig. 10. Tests in treated-milk samples for sensors with only buffer solution in milk (M), with LL (M + LL), and with LL phage contamination (M + LL + PG). (a) Optical absorbance versus the time. (b) Normalized charge transfer resistance R_{ct}/R_{ct0} extrapolated by the EIS measurements. (c) Differential phase at 400 Hz extrapolated by the EIS measurements. The error bars of the black curves are small and covered by the size of the markers.

progresses, and, thus, the bacteria are able to cover almost all the electrode surface, the phase decreases more evidently in LL sensors. After 240 min, the LL and PG phase curves are clearly distinguishable. At 270 min, the phase difference is 46° for the LL sensors versus 24° for the PG sensors, thus demonstrating that the phase is also a good discriminative parameter for detecting the bacterial growth and the presence of phages in solution.

Thus, the detection principle of the proposed biosensor is based on differential measurements between a reference LL solution and a sample to test. The different trends of LL and LL + PG curves allow to distinguish the contaminated solution from the phage-free sample, effectively detecting the presence of phages in about 4 h, which is at least 1 h less than other methods presented in the literature, typically requiring testing times >6 h [3], [19].

D. Milk-Based Samples

We carried out experimental test and validation using milk-based samples, getting closer to a real-life application. The milk was filtered to remove the fat content and to precipitate the casein. The milk filtering protocol consisted in the centrifugation of raw milk at 10 000 r/min for 5 min; then, the supernatant (pH 6.5) was extracted. In order to precipitate the casein, the pH was lowered to 4.6 by adding 37% HCl. The obtained solution was again centrifuged at 10 000 r/min for 5 min, filtered with a 0.22-μm filter and then stored in the fridge. The phages test solution was prepared by adding 240 μL of filtered milk to 240 μL of phages in PB, while the control solution and the solution with LL were obtained with 240 μL of filtered milk and 240 μL of PB (without phages).

Fig. 9 reports the Nyquist curves and phase of EIS responses of three different biosensors tested with filtered-milk-based solutions. The M sensor (continuous line) was tested with only the buffer solution in filtered milk. The M + LL sensor was tested with treated milk solution containing the LL bacteria. Also, the M + LL + PG sensor was tested with the LL bacteria and with 10^7 PFU/mL of phages. The M curve evidences a slight shift between 0 (black curve) and 300 min (red curve). This shift is higher than the one retrieved for ideal M17 solution [see Fig. 7(a)], most likely due to the deposition of some residual milk components on the electrode surface, which contribute to the increase in R_{ct}. The highest shift is detected in the M + LL sensor, exhibiting large parametrical shift at 300 min, similar to the LL of Fig. 6. The M + LL + PG curve at 300 min is still clearly characterized by the semicircle at medium frequencies. The large difference between the M + LL + PG and M + LL sensors demonstrated the sensing capability of the proposed method also in the presence of filtered milk.

Fig. 10 summarizes the parametrical shifts as a function of the time with solutions prepared with treated milk. In Fig. 10(a), the absorbance curve of the only treated milk is approximately stable around 0 along the entire experiment time, confirming the nonproliferation of other external undesired bacteria. The M + LL and M + LL + PG curves increase exponentially in the first 90 min with similar trends. After 90 min, the absorbance value of the M + LL sensors continues its rapid increase, while the M + LL + PG sensors have a rebound, which decreases the OD values to about 0.02 after 210 min. The fall of the OD values of the M + LL + PG sensors indicates that the phage activity dominates the bacterial growth, until its complete inhibition.

This difference between the M + LL and M + LL + PG sensors is similarly visible from the normalized R_{ct} values after 210 min [see Fig. 10(b)]. At 210 min, R_{ct}/R_{ct0} of M + LL sensors is 2.5 versus 1.8 of the M + LL + PG sensors. The dotted arrow visible for the M + LL curve indicates an explosion of R_{ct}, which increases more than one order of magnitude after 270 min, similar to Fig. 8(b). On the other hand, R_{ct} of M + LL + PG sensors increases just to 2.6 at 300 min, consistent with an extremely limited growth of the LL, and consistent with the absorbance measurements.

The different responses between M + LL + PG and M + LL sensors are particularly evident in the impedance phase. Fig. 10(c) shows the phase shifts at 400 Hz. After 210 min, the M + LL phase decreases more evidently than the

M + LL + PG curve, which, in turn, starts to settle around −19°. After 300 min, the phase shift for the M + LL sensors (green dashed curve) is −19°, while the M + LL + PG sensor (red dotted curve) shows a phase value of −43°, leading to an overall difference of about 24° between the filtered milk solutions contaminated and uncontaminated by phages.

These tests evidence that the proposed sensor is capable of effectively detecting the presence of phages even in a solution closer to a real sample in less than 5 h. These results represent the proof of concept of the proposed LL phages detection method and may pave a valuable way for future work on the device performance optimization and in real milk environments.

V. Summary and Conclusion

In this work, we have proposed a new electrochemical biosensor capable of detecting the LL bacteriophages. Electrochemical tests evidence that the best stable devices are the commercial screen-printed electrodes made in gold and silver with high repeatability and stability over the time and to the cleaning procedures.

The biosensing idea is based on the spill-out technique, which consists in the deposition of a drop of solution containing live LL bacteria on the sensor electrodes. The relatively fast precipitation of the bacteria on the electrodes causes the formation of a thin layer of bacteria over the sensor electrodes, which decreases the transport of electrons at the electrode/solution interface, thus raising the charge transfer resistance. The bacterial growth is measured through EIS, showing an evident increase in charge transfer resistance and a decrease in the impedance phase at 400 Hz. On the other hand, samples infected by the phages inhibit the bacterial growth and have low concentrations of bacteria, leading to significantly lower shifts of the electrical parameters. The phase variation at 400 Hz has proven to be an optimal discriminative parameter for the detection of bacteriophages with a shift of about 23° for detecting 10^7 PFU/mL of phages. Another advantage of the phase variation is the relatively easy measurement, which requires an impedance measurement just at a single frequency. The biosensor was tested in ideal solutions and with filtered milk samples, yielding similar and promising results for both conditions in less than 5 h.

Future work will aim to the performance optimization and to validate the method with solutions closer to real ones. Comprehensive studies will be necessary to understand the influence of other perturbative external factors, as temperature, as well as the possibility to simplify the biosensing process at minimum, such as the milk treatment. Overall, the proposed biosensor may pave a faster and cheaper detection of bacteriophages compared with the traditional laboratory approaches, being also promising for the detection of other types of phages.

References

[1] F. Rossi, "Microbiology in dairy processing: Challenges and opportunities," *Chall*, vol. 9, no. 1, p. 8, Feb. 2018.

[2] J. E. Garneau and S. Moineau, "Bacteriophages of lactic acid bacteria and their impact on milk fermentations," *Microbial Cell Factories*, vol. 10, no. 1, p. S20, 2011.

[3] B. del Rio, A. G. Binetti, M. C. Martín, M. Fernández, A. H. Magadán, and M. A. Alvarez, "Multiplex PCR for the detection and identification of dairy bacteriophages in milk," *Food Microbiol.*, vol. 24, no. 1, pp. 75–81, Feb. 2007.

[4] A. Saravanan et al., "Methods of detection of food-borne pathogens: A review," *Environ. Chem. Lett.*, vol. 19, pp. 189–207, Aug. 2020.

[5] L. Rotariu, F. Lagarde, N. Jaffrezic-Renault, and C. Bala, "Electrochemical biosensors for fast detection of food contaminants–trends and perspective," *TrAC Trends Anal. Chem.*, vol. 79, pp. 80–87, May 2016.

[6] N. Kalyani, S. Goel, and S. Jaiswal, "On-site sensing of pesticides using point-of-care biosensors: A review," *Environ. Chem. Lett.*, vol. 19, pp. 345–354, Sep. 2020.

[7] E. R. Richter, "Biosensors: Applications for dairy food industry," *J. Dairy Sci.*, vol. 76, no. 10, pp. 3114–3117, Oct. 1993.

[8] G. Mishra, A. Barfidokht, F. Tehrani, and R. Mishra, "Food safety analysis using electrochemical biosensors," *Foods*, vol. 7, no. 9, p. 141, Sep. 2018.

[9] K. Rathee, V. Dhull, R. Dhull, and S. Singh, "Biosensors based on electrochemical lactate detection: A comprehensive review," *Biochem. Biophys. Rep.*, vol. 5, pp. 35–54, Mar. 2016.

[10] G. Rosati, M. Ravarotto, M. Scaramuzza, A. De Toni, and A. Paccagnella, "Silver nanoparticles inkjet-printed flexible biosensor for rapid label-free antibiotic detection in milk," *Sens. Actuators B, Chem.*, vol. 280, pp. 280–289, Feb. 2019.

[11] T. Rinken and H. Riik, "Determination of antibiotic residues and their interaction in milk with lactate biosensor," *J. Biochem. Biophys. Methods*, vol. 66, nos. 1–3, pp. 13–21, Mar. 2006.

[12] D. L. Alecandre et al., "A rapid and specific biosensor for Salmonella Typhimurium detection in milk," *Food Bioprocess Technol.*, vol. 11, pp. 748–756, Jan. 2018.

[13] H. Yang, H. Zhou, H. Hao, Q. Gong, and K. Nie, "Detection of Escherichia coli with a label-free impedimetric biosensor based on lectin functionalized mixed self-assembled monolayer," *Sens. Actuators B, Chem.*, vol. 229, pp. 297–304, Jun. 2016.

[14] M. Manzano, S. Viezzi, S. Mazerat, R. S. Marks, and J. Vidic, "Rapid and label-free electrochemical DNA biosensor for detecting hepatitis a virus," *Biosensors Bioelectron.*, vol. 100, pp. 89–95, Feb. 2018.

[15] F. Li, "An ultrasensitive CRISPR/Cas12a based electrochemical biosensor for Listeria monocytogenes detection," *Biosensors Bioelectron.*, vol. 179, May 2021, Art. no. 113073.

[16] I. Grabowska, K. Malecka, U. Jarocka, J. Radecki, and H. Radecka, "Electrochemical biosensors for detection of avian influenza virus–current status and future trends," *Acta Biochim. Pol.*, vol. 61, no. 3, pp. 471–478, 2014.

[17] M. C. García-Anaya, D. R. Sepulveda, A. I. Sáenz-Mendoza, C. Rios-Velasco, P. B. Zamudio-Flores, and C. H. Acosta-Muñiz, "Phages as biocontrol agents in dairy products," *Trends Food Sci. Technol.*, vol. 95, pp. 10–20, Jan. 2020.

[18] Y. Chai, S. Li, S. Horikawa, M.-K. Park, V. Vodyanoy, and B. A. Chin, "Rapid and sensitive detection of Salmonella typhimurium on eggshells by using wireless biosensors," *J. Food Protection*, vol. 75, no. 4, pp. 631–636, Apr. 2012.

[19] C. García-Aljaro, X. Muñoz-Berbel, and F. J. Muñoz, "On-chip impedimetric detection of bacteriophages in dairy samples," *Biosensors Bioelectron.*, vol. 24, no. 6, pp. 1712–1716, Feb. 2009.

[20] G. Rosati et al., "A plug, print & play inkjet printing and impedance-based biosensing technology operating through a smartphone for clinical diagnostics," *Biosensors Bioelectron.*, vol. 196, Jan. 2022, Art. no. 113737.

[21] R. Young, "Bacteriophage lysis: Mechanism and regulation," *Microbiol. Rev.*, vol. 56, no. 3, pp. 430–481, Sep. 1992.

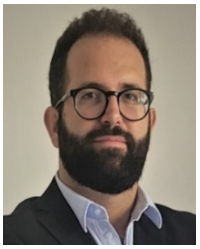

Stefano Bonaldo (Member, IEEE) received the M.Sc. degree in electronic engineering and the Ph.D. degree in information engineering from the University of Padova, Padua, Italy, in 2016 and 2020, respectively.

He was a Ph.D. Visitor Student with Vanderbilt University, Nashville, TN, USA, for one year. Since 2020, he has been a Postdoctoral Researcher with the Department of Information Engineering, University of Padova. His research interests include the development of innovative electrochemical biosensors and their electrical modeling with applications in the medical and agrifood sectors, and the exploration of radiation effects in ultrascaled CMOS technologies for space and high-energy physics applications.

Erica Cretaio received the M.Sc. degree in medical biotechnology and the Ph.D. degree in biochemistry and biotechnology from the University of Padova, Padua, Italy, in 2004 and 2008, respectively.

She is the CEO of ARCADIA s.r.l., Padua, where she is involved in the technical activity. Her research interests include the design and setup of biosensing platforms for medical diagnosis and follow-up, environmental and microbiological monitoring of food and water, molecular and cellular biology, biochemistry and microbiology, biocompatibility, biosafety, and antimicrobial or antitumor activity of innovative materials.

Elisabetta Pasqualotto received the M.Sc. degree in bioengineering and the Ph.D. degree in information science and technology from the University of Padova, Padua, Italy, in 2009 and 2014, respectively.

She has been a Postdoctoral Researcher with the Department of Information Engineering, University of Padova, since 2015, and the Co-Founder and the Technical Manager of ARCADIA s.r.l., Padua, and other technological start-ups. Her main research interests during the Ph.D. and postdoctoral period include the study and the development of sensors for medical and biological applications. Part of her research activity has been carried out to develop an innovative laboratory-on-chip manufacturing process, and design and test the novel low-cost grating-based devices for surface plasmon resonance (SPR) and electrochemical analysis.

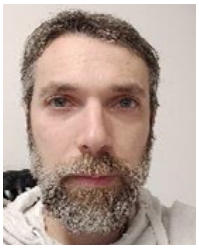

Matteo Scaramuzza (Member, IEEE) received the M.Sc. degree in electronic engineering and the Ph.D. degree in science and information from the University of Padova, Padua, Italy, in 2010 and 2014, respectively.

He is the Co-Founder of the ARC-Centro Ricerche Applicate, Padua, and other technological start-ups. He is listed as an inventor in different international patents related to life science technologies and novel manufacturing processes. His research and technological interests include solid-state sensors for gases and analytes, electrochemical and optoelectronic sensors and biosensors, sensing applications of light, and biometric parameters transducers.

Lara Franchin received the M.Sc. degree in bioengineering from the University of Padova, Padua, Italy, in 2022, where she is pursuing the Ph.D. degree with the Department of Information Engineering.

Her research interests include the development and validation of electrochemical biosensors with applications in the medical and agrifood sectors.

Sara Poggi received the M.Sc. degree in electronic engineering from the University of Padova, Padua, Italy, in 2022. During her master's thesis, she focused on the development of electrochemical biosensors for the detection of pathogens in the agri-food sector.

Recently, she has joined DB Elettronica e Telecomunicazioni s.r.l., Padova, as a Radio Frequency Designer.

Alessandro Paccagnella (Senior Member, IEEE) was a Vice Rector for international relations of the University of Padova, Padua, Italy, from 2015 to 2021, being in charge for managing the international relations of the university. He is a Full Professor of Electronics with the Department of Information Engineering, University of Padova. He is also an Honorary Professor with the Institute of Microelectronics of the Chinese Academy of Sciences, Beijing, China. Since few years, he has started a new research activity in the field of biosensors, with attention to both the fabrication of devices and to the implementation of accurate modeling of the complex system, lately including new electrochemical and plasmonic sensors for microfluidic applications. He is developing new technological platforms for sensors, aiming to achieve low-cost devices for screening applications in a variety of fields, including medical, food quality, and environmental pollution. In the scientific field, his research interests include microelectronic devices and systems.

Open Access funding provided by 'Università degli Studi di Padova' within the CRUI CARE Agreement